NeuroImage: Clinical 22 (2019) 101689

Contents lists available at ScienceDirect

NeuroImage: Clinical

journal homepage: www.elsevier.com/locate/ynicl

Anodal tDCS modulates cortical activity and synchronization in Parkinson's disease depending on motor processing

Anna Schoellmann[a,b,*], Marlieke Scholten[a,b], Barbara Wasserka[c], Rathinaswamy B. Govindan[d], Rejko Krüger[a,b,e,f], Alireza Gharabaghi[e,g], Christian Plewnia[c,e], Daniel Weiss[a,b,*]

[a] Center for Neurology, Department for Neurodegenerative Diseases, Hertie Institute for Clinical Brain Research, University of Tübingen, Hoppe-Seyler-Str. 3, 72076 Tübingen, Germany
[b] German Center for Neurodegenerative Diseases (DZNE), Otfried-Müller-Straße 23, 72076 Tübingen, Germany
[c] Neurophysiology & Interventional Neuropsychiatry, Department of Psychiatry and Psychotherapy, University of Tübingen, Calwerstr. 14, 72076 Tübingen, Germany
[d] Foetal Medicine Institute, Division of Foetal and Transitional Medicine, Children's National Health System, M3118C Washington, DC, USA
[e] Werner-Reichardt Centre for Integrative Neuroscience, 72076 Tübingen, Germany
[f] Clinical and Experimental Neuroscience, Luxembourg Center for Systems Biomedicine (LCSB), University of Luxembourg and Centre Hospitalier de Luxembourg (CHL), 1210 Luxembourg, Luxembourg
[g] Division of Functional and Restorative Neurosurgery, Department of Neurosurgery, University of Tübingen, Hoppe-Seyler-Str. 3, 72076 Tübingen, Germany

ARTICLE INFO

Keywords:
Parkinson's disease
brain stimulation
transcranial direct current stimulation
cortical
coherence

ABSTRACT

Background: Transcranial direct current stimulation (tDCS) may alleviate motor symptoms in Parkinson's disease (PD). However, the neurophysiological effects of tDCS on cortical activation, synchronization, and the relation to clinical motor symptoms and motor integration need characterization.
Objective: We aimed to explore the effect of tDCS over the left sensorimotor area on clinical motor outcome, right hand fine motor performance as well as cortical activity and synchronization in the high beta range.
Methods: In this double-blind randomized sham-controlled clinico-neurophysiological study we investigated ten idiopathic PD patients and eleven matched healthy controls (HC) on two days during an isometric precision grip task and at rest before and after 'verum' and 'sham' anodal tDCS (20 min; 1 mA; anode [C3], cathode [Fp2]). We measured clinical outcome, fine motor performance, and analysed both cortical frequency domain activity and corticocortical imaginary coherence.
Results: tDCS improved PD motor symptoms. Neurophysiological features indicated a motor-task-specific modulation of activity and coherence from 22 to 27 Hz after 'verum' stimulation in PD. Activity was significantly reduced over the left sensorimotor and right frontotemporal area. Before stimulation, PD patients showed reduced coherence over the left sensorimotor area during motor task compared to HC, and this increased after 'verum' stimulation in the motor task. The activity and synchronization modulation were neither observed at rest, after sham stimulation nor in healthy controls.
Conclusion: Verum tDCS modulated the PD cortical network specifically during fine motor integration. Cortical oscillatory features were not in general deregulated in PD, but depended on motor processing.

1. Introduction

Neuronal activity and synchronization of cortical and subcortical circuits support the dynamic functional interplay of different brain areas and integration of complex cognitive functions including motor processing (Neuper et al., 2006; Pfurtscheller and Lopes, 1999). Maladaptive neuronal oscillatory activity and synchronization provide relevant features of neuropsychiatric disease including Parkinson's disease (PD) (Hammond et al., 2007; Uhlhaas and Singer, 2006; Weiss et al., 2015). In PD, increased activity in the beta frequency range in the

Abbreviations: APB, abductor pollicis brevis muscle; atDCS, anodal tDCS; DBS, deep brain stimulation; FDI, first dorsal interosseous muscle; GABA, gamma-aminobutyric acid; HC, healthy controls; MAD, mean absolute deviation; PD, Parkinson's disease; SM1, primary sensorimotor area; M1, primary motor area; rmANOVA, repeated measures analysis of variance; Ag/AgCl, silver/silver chloride; STN, subthalamic nucleus; tACS, transcranial alternating current stimulation; tDCS, transcranial direct current stimulation; UPDRS, Unified Parkinson's disease rating scale

* Corresponding authors at: Center for Neurology, Department for Neurodegenerative Diseases, Hertie Institute for Clinical Brain Research, University of Tübingen, Hoppe-Seyler-Str. 3, 72076 Tübingen, Germany.
E-mail addresses: anna.schoellmann@med.uni-tuebingen.de (A. Schoellmann), daniel.weiss@uni-tuebingen.de (D. Weiss).

https://doi.org/10.1016/j.nicl.2019.101689
Received 29 August 2018; Received in revised form 21 January 2019; Accepted 22 January 2019
Available online 23 January 2019

Table 1
Clinical characteristics of Parkinson's disease patients.

ID	Sex/Age, years	Disease duration, years	Disease-dominant hand	Main symptom	Levodopa equivalent dose, mg/d
1	M/56	8	R	Bradykinesia, rigidity	800
2	F/74	10	L	Bradykinesia, rigidity	1410
3	M/61	7	L	Bradykinesia, rigidity	844
4	F/46	5	R	Bradykinesia, rigidity	0
5	M/74	19	R	Bradykinesia, rigidity	1000
6	F/60	11	L	Bradykinesia, rigidity	1050
7	M/50	8	R	Bradykinesia, rigidity	657.5
8	M/70	8	R	Bradykinesia, rigidity	870
9	M/72	7	R	Bradykinesia, rigidity	600
10	F/80	3	R	Bradykinesia, rigidity	260

Abbreviations: ID, Identity; M, male, F, female; R, right, L, left.

subthalamic nucleus (STN) may parallel rigidity and bradykinesia (Hammond et al., 2007; Brown, 2007; Gaynor et al., 2008; Kuhn et al., 2006; Tinkhauser et al., 2017a). Dopaminergic medication as well as deep brain stimulation of the STN may normalize these oscillatory features in parallel to clinical improvement (Tinkhauser et al., 2017b; Kuhn et al., 2008). However, pathological synchronization is not restricted to the basal ganglia, but entrains cortical motor networks through local activation changes and long-range synchronization in striato-thalamo-cortical circuits (Silberstein et al., 2005; Potter-Nerger et al., 2008; Benninger and Hallett, 2015; Wichmann et al., 2011; Tinkhauser et al., 2018; van Wijk et al., 2016). Clinical symptoms may relate to malfunction of the subcortico-cortical motor circuit (Litvak et al., 2011). As such, the subcortico-cortical motor network seems to comprise of different functional loops in which functional segregation is achieved through topographic distribution but also selective coupling at different frequencies (Lalo et al., 2008). Interregional coupling between STN and motor cortex (M1) in the beta band seems to be concentrated into bursts and can be modulated with dopaminergic medication and subthalamic neurostimulation (Tinkhauser et al., 2018; van Wijk et al., 2016; Litvak et al., 2011; Oswal et al., 2016). In this sense, it is of interest, whether there is also cortical ('non-invasive') access to restore the multistage subcortico-cortical motor network failure in order to improve clinical outcome (Gaynor et al., 2008). By stimulating the cortical motor circuit, brain stimulation techniques might provide safe and easy access to the PD STN-M1 motor circuit (Gaynor et al., 2008). In addition this might help to improve the pathophysiological understanding of PD as well as the neurophysiological mechanisms underlying clinical motor symptom response to cortical stimulation (Benninger and Hallett, 2015; Lefaucheur et al., 2004; Lefaucheur et al., 2017). To this end, transcranial direct current stimulation (tDCS) delivers a continuous current that may modulate neuronal excitability and oscillatory cortical features (Lefaucheur et al., 2017; Priori et al., 1998; Nitsche and Paulus, 2000, 2001; Floel, 2014; Roy et al., 2014; Polania et al., 2011, 2012; Keeser et al., 2011a, 2011b; Fregni et al., 2006). Imaging studies indicate that tDCS may also modulate functional activity and connectivity within and between different brain regions (Polania et al., 2011; Baudewig et al., 2001; Lang et al., 2005). Several studies showed motor improvement in PD after atDCS over motor regions (Lefaucheur et al., 2017; Fregni et al., 2006; Verheyden et al., 2013; Valentino et al., 2014; Pascual-Leone et al., 1994; Ferrucci et al., 2016; Dagan et al., 2018; Costa-Ribeiro et al., 2016; Costa-Ribeiro et al., 2017; Benninger et al., 2010). Apparently, neuronal networks respond sensitively to DC fields (Lefaucheur et al., 2017; Francis et al., 2003) and excitability changes outlast the stimulation period and become steadily significant after the end of application (Nitsche and Paulus, 2001; Nitsche et al., 2003; Santarnecchi et al., 2014).

In contrast to the manifold studies on the modulation of oscillatory frequency features of the beta range by deep brain stimulation, the effect of tDCS on cortical activity and synchronization within the motor network in PD is less understood.

In this study, we aim to characterize the clinical after-effect of atDCS on PD motor symptoms and cortical oscillatory activity and synchronization. We postulate that stimulation of the sensorimotor area will not only modulate local neuronal activity, but also entrain network-wide changes in activity and synchronization of the cortical motor network.

2. Materials and methods

2.1. Patients

In this double-blind randomized sham-controlled study, we investigated eleven medically treated PD patients (seven male, age 64.3 ± 11.4, disease duration 8.6 ± 4.1) and ten healthy controls (HC) (six male, age 58.6 ± 6.8) matched for age (independent samples *t*-test; $p = .193$) and gender (Chi^2- test; $p = 1$) (patient characteristics in Table 1).

One patient (PD11) was excluded as the patient was unable to cooperate after withdrawal of medication. All participants provided written informed consent. The study was approved by the local ethics committee of the University of Tübingen (367/2010BO1). PD patients were studied in motor 'OFF' after overnight withdrawal (at least 12 h) of dopaminergic medication.

We included right-handed subjects (Oldfield, 1971) with age > 18– < 80 years. We excluded patients with dementia, other neuropsychiatric disease or other severe medical conditions. Moreover, we excluded patients with dyskinesia and preferred such without tremor. If tremor appeared unexpectedly during the recordings, we rejected the respective time series. We also obtained the Mini Mental State Examination Score and Beck's Depression Inventory (Folstein et al., 1975; Beck et al., 1996). PD and HC were investigated during an isometric precision grip task of the right index finger and thumb (Weiss et al., 2012).

2.2. Experimental design, study protocol, paradigm

A schematic overview of the study protocol is given in Fig. 1. Briefly, we studied two groups ['*PD*', '*HC*'] in two stimulation conditions ['*verum*', '*sham*' atDCS] before ('pre'), immediately after ('post1'), and 30 min after ('post2') stimulation. The stimulation conditions were administered on two separate days, and stimulation was delivered in double-blind manner and randomized order. At each timepoint, patient received a recording during performance of an isometric motor precision task and at rest.

tDCS ring electrodes (7.5 cm diameter; 37 cm^2; neuroConn GmbH, Ilmenau, Germany) were placed over the left sensorimotor [C3, anode] and right frontal areas [Fp2, cathode] (Nitsche and Paulus, 2000). For 'verum' stimulation (DC-stimulator Plus ®, neuroConn GmbH, Ilmenau, Germany), we administered a continuous current for 20 min with 1 mA. In 'sham', active stimulation with 1 mA was discontinued after 40s. Both conditions had a linear 5 s fade-in/−out period at the beginning and end of stimulation (Ambrus et al., 2012), in order to enable valid

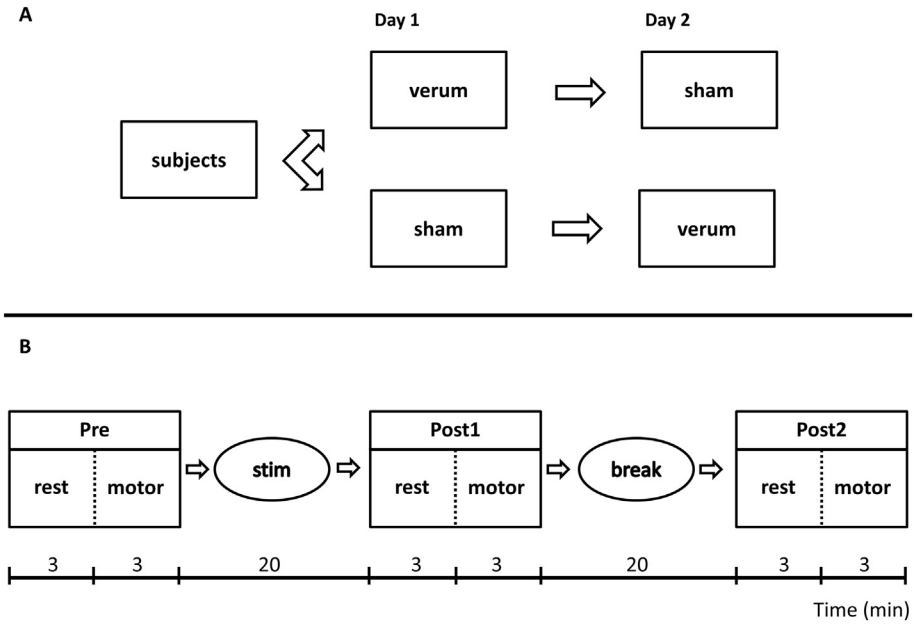

Fig. 1. Study protocol.
A: All subjects received verum and sham stimulation in random order. We administered the stimulation conditions (verum; sham) on two separate days in in double-blind manner.
B: timeline of one experimental day with three sessions: 'pre' (before stimulation), 'post1' (directly after stimulation) and 'post2' (30 min after stimulation). In each session, we recorded EEG and EMG at rest and during performance of an isometric motor precision task.

placebo control (Palm et al., 2013). Current density was kept below 0.1 mA/cm^2 and impedance was kept below 6 kΩ.

2.3. Clinical motor outcome and fine motor performance

We recorded clinical motor symptoms in 'pre', 'post1' and 'post2' as UPDRS III motor score (hemibody score, sum of items 22–25, right hand contralateral to 'C3' anodal stimulation side).

For the fine motor assessment, participants performed a precision grip task with an isometric contraction of their right index finger and thumb and visual feedback on a computer screen for the calibration period as described elsewhere (Weiss et al., 2012). The force level was measured with a mechanogram with a sampling rate of 1000 Hz. Visual congruency of two rectangles represented ideal calibration of the current force level $Force_{curr}$ to the defined force level of 2 N. Subjects received a calibration period of 10s. Then, visual feedback was withdrawn for 14 s and subjects had to maintain the calibrated force level followed by a 7 s interval to relax their hand on the armrest. Only the data without visual feedback during the precision grip task was used for further analysis. Blocks of 1–3 min length were obtained and used for further analysis. We excluded time series in which the subject did not adhere to the paradigm (e.g. not pressing or missing pre-calibration period).

The accuracy error of fine motor performance was expressed as mean absolute deviates (MAD), where x_i is the value of the difference between 2 Newton and the current force level $Force_{curr}$ at the sampling point i (Trenado et al., 2014). We used the sum of the absolute value of x_i devided by n (number of samples of the respective time series). MAD values were log-transformed (Trenado et al., 2014). There was no bias of the MAD due to different block lengths.

$$MAD = \frac{1}{n}\sum_{i=1}^{n}|x_i|, \text{ where, } x = 2Newton - Force_{curr} \quad (1)$$

2.4. Electrophysiological recordings

We obtained surface EEG (Neuro Prax ® tES, NeuroConn) with Ag/AgCl electrodes (EASYCAP, GmbH Herrsching, Germany) using the left earlobe as reference electrode and a frontal electrode as ground [AF3]. Electrodes were placed according to the 10–20 system using standardized caps (EASYCAP, GmbH Herrsching, Germany) (Klem et al., 1999), and EEG was obtained from 25 channels. In addition, the EMG was recorded from the right abductor pollicis brevis (APB) and first dorsal interosseous (FDI) muscles with references over the distal interphalangeal joint of the thumb (for the APB) and the distal interphalangeal joint of the index finger (for the FDI) (McAuley et al., 1997). In this work, we focus on EEG analysis including measures of cortical activity and corticocortical synchronization. Time series were sampled at 1000 Hz.

2.4.1. Preprocessing

We filtered the EEG data (finite impulse response filter; pass band 1-200 Hz; 45–55 Hz notch for line artefact) with zero-phase distortion and compensation for group delay. We inspected EEG data visually and rejected muscle and movement artefacts as well as few episodes in which tremor was detected on kinematic or EMG time series. Further transient artefacts (eye-movement, eye blinking, cardiovascular) were removed with a principal component analysis. Then, we transformed the time series back to channel space. We converted the EEG data with Hjorth transformation in order to reduce the potential influence of volume conduction and in order to improve spatial resolution (Hjorth, 1991; Kayser and Tenke, 2015). For the Hjorth transformation, we used a neighbour file with 4–6 neighbours per electrode depending on the localization of the electrode. Only electrodes in direct proximity to each other qualified as neighbour and standardized EEG caps determined the distances between electrodes. All analyses were performed off-line with MATLAB 7.14 (R2012a) (The MathWorks, Natick, MA, USA) using the *open-source toolboxes* EEGlab (v13.1.1b) (Delorme and Makeig, 2004) and Fieldtrip (Oostenveld et al., 2011).

2.4.2. Frequency domain spectrum of cortical activity

We expressed cortical activity as frequency domain spectrum (power) and obtained the topographic distribution from the cortical channels. Therefore, we divided EEG data into rectangular, non-overlapping 1-second windows (frequency resolution of 1 Hz). Spectral estimation was performed using the Welch periodogram approach. In this approach, the EEG signals were segmented into 1 s (Fourier transform length) epochs. For data in each epoch, a periodogram was calculated as the square of the magnitude of the Fourier transform of the data. To this end, the spectral estimate was calculated by averaging the periodograms over all epochs (we used 100 epochs in each subject for further analysis). The inverse of the Fourier transform length fixed the frequency resolution of the power spectrum. The reference for the

relative measure (spectral power) is the total power (1–100 Hz). The relative spectral activity in a specific frequency band is defined as the ratio of the sum of spectral power in that specific frequency band to the sum of the spectral power between 1 and 100 Hz.

2.4.3. Corticocortical connectivity with imaginary coherence

As a parameter for synchronised activity between two brain regions, we computed the imaginary corticocortical coherence (Nolte et al., 2004) spectra from the same data segments (100 s of data) as the activity. We used the imaginary part of coherence since it is considered insensitive to spurious non-neuronal connectivity from zero-phase delayed volume conduction (Nolte et al., 2004).

2.5. Statistical analyses

2.5.1. Clinical outcome and fine motor performance

Clinical motor outcome was analysed in the PD group as 2 × 3 repeated measures analysis of variance (rmANOVA) with the main within-subject factors CONDITION ('verum', 'sham') and SESSION ('pre', 'post1', 'post2'). Fine motor performance was analysed using a 3 × 2 × 2 rmANOVA with the within-subject factors SESSION (pre/post1/post2), CONDITION (verum/sham) and the between-subject factor GROUP (PD/HC). Homogeneity between groups was tested with Levene's test. We applied Huynh-Feldt or Greenhouse-Geisser correction in case the sphericity assumption in the Mauchly's test was violated. Shapiro-Wilk test was used to test for normal distribution of the data. The confidence interval was set to 95% and hypotheses were decided on a two-tailed $P \leq .05$. We used paired *t*-tests and Bonferroni correction for post hoc analysis in case of significant interactions.

2.5.2. Activity and imaginary corticocortical coherence in the beta frequency range

We explored cortical activity and imaginary coherence during the 'motor task'. Similar to the statistical analysis of the 'motor task', we also performed statistical analysis of the time series 'at rest'. As the approach is similar, the detailed description of these analyses in the following section will apply to both 'motor task' and 'at rest'.

Exploration of the data during the motor task pointed to activation changes in a circumscribed subrange of the high beta band from 22 to 27 Hz. This frequency range selection differs from traditional pre-defined frequency bands that traditionally do not stem from the pathophysiological PD context. Meaningful disease-related subranges were described in smaller sub-bands of the broad beta range between 13 and 30 Hz (Tinkhauser et al., 2017a; Kuhn et al., 2008; Silberstein et al., 2005; Eusebio et al., 2011; Pogosyan et al., 2009). For comparison, subranges of the high beta range were implicated in cross-site synchrony and subcortico-cortical networks in PD (Tinkhauser et al., 2018; Oswal et al., 2016). In line with this consideration, two functionally distinct oscillatory beta activities in subcortico-cortical networks were suggested: one centered at around 15 Hz and another around 25 Hz (Tinkhauser et al., 2018; van Wijk et al., 2016; Litvak et al., 2011), which might reflect two sub-circuits susceptible to episodes of exaggerated coupling (Oswal et al., 2016).

Since we placed our anodal stimulation electrode over the sensorimotor area, we had the specific hypothesis to modulate the sensorimotor area ('C3') with 'verum' atDCS in PD. To this end, we used a 3 × 2 × 2 rmANOVA with the within-subject factors SESSION (pre/post1/post2), CONDITION (verum/sham) and between-subject factor GROUP (PD/HC). Homogeneity between groups was confirmed with Levene's test (all n.s.). We applied Huynh-Feldt or Greenhouse-Geisser correction in case the sphericity assumption in the Mauchly's test was violated. Shapiro-Wilk test was used to test for normal distribution of the data. In addition, we explored the cortical distribution of activity and corticocortical coherence (average of 22–27 Hz). We compared the sessions 'pre' and 'post2' and excluded 'post1' from the statistical spectral analysis to limit the number of comparisons (channels (25), conditions (2), sessions (3)) (Maris, 2012; Maris and Oostenveld, 2007). This data reduction approach is also justified from a clinical standpoint, since i) we aimed to study the electrophysiological correlate of a stable after-effect from atDCS and ii) the clinical changes induced by atDCS outlasted 'post1' and still persisted in 'post2' in this work. In detail, cortical activity and corticocortical coherence were compared i) between 'pre' and 'post2' in both PD and HC and ii) between groups in the 'pre' session using a cluster-based permutation test as implemented in *Fieldtrip* to address for multiple comparisons (Oostenveld et al., 2011). This test is based on the Monte-Carlo principle and recognizes significant changes between conditions using spatial adjacency by building clusters of channels. We used 5000 random permutations on a dependant samples *t*-test (comparing session 'pre' vs. 'post2') or 2 × 2 independent samples *t*-test (comparing HC vs. PD before stimulation) and an adjusted alpha level of $P < .025$ per tail. As these sample-wise t-test statistics produce a high number of comparisons, the cluster-based correction method is effective to treat the multiplicity problem without losing sensitivity for spectral modulations (Weiss et al., 2015; Oostenveld et al., 2011).

2.5.3. Disease-related differences between groups

For activity and coherence analysis, we compared the groups before stimulation [HC 'pre' vs. PD 'pre'] to explore for disease-related differences. We averaged the 'pre' data in each group, after ensuring that verum and sham before stimulation ('pre verum' vs. 'pre sham') did not differ significantly (paired t-test, all n.s.). Activity and coherence in the high beta band [22–27 Hz] were plotted for the whole cortex and difference plots were computed. Again, permutation statistics were used as explained in 2.5.2 (Oostenveld et al., 2011).

3. Results

3.1. Clinical outcome and fine motor performance

PD patients showed clinical motor improvement of the segmental UPDRS III hemibody subscore of the right hand (task 22–25) after verum stimulation (post1), and this lasted for at least 30 min (post2) (Fig. 2; 'condition' [$F = 5.884$, $p = .038$], 'session' [$F = 14.270$,

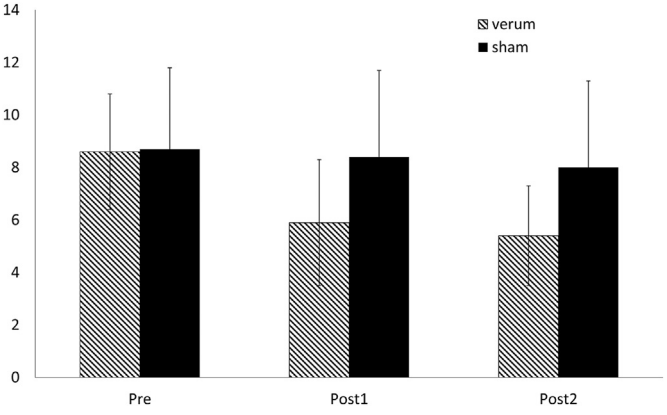

Fig. 2. Motor improvement after verum stimulation in PD.
Motor UPDRS III hemibody score of the right upper extremity (items 22–25) in PD before and after stimulation in verum-condition compared to sham-condition (mean ± SD).
The 3 × 2 rmANOVA of this score with the factors 'session' [pre, post1, post2] and 'condition' [verum; sham] showed significant findings for 'condition' [$F = 5.884$, $p = .038$], 'session' [$F = 14.270$, $p < .001$] and 'condition*session' [$F = 11.292$, $p = .004$] (all Huynh-Feldt corrected). The post-hoc analysis including Bonferroni correction showed a difference on verum 'pre vs. post1': $t = 4.801$, $p = .001$ and verum 'pre vs. post2': $t = 7.236$, $p = .000$. We found no difference for sham 'pre vs. post1': $t = 1.105$, $p = .298$ and sham 'pre vs. post2': $t = 0.669$, $p = .520$.

p < .001] and 'condition*session' [F = 11.292, p = .004]). The post-hoc analysis showed a difference on verum 'pre vs. post1': confidence interval [2.19964–4.20036], t = 4.801, p = .001 and verum 'pre vs. post2': confidence interval [0.80548–4.19452], t = 7.236, p = .000. We found no difference for the same post-hoc contrasts in 'sham' (all n.s.). However, we observed a marginal reduction of mean UPDRS III outcome in sham condition over time, which did not show statistical significance. We additionally contrasted the effect of sham condition [sham_post2 – sham_pre] with the effect of verum condition [verum_post2 – verum_pre]. Here, we found a significant difference [sham (post2-pre) vs. verum (post2-pre): confidence interval [0.80548 4.19452], t = 3.337, p = .009 (paired t-test)], which means that the verum effect cannot be explained by the small difference between the pre and post2 sessions in sham condition. The pre-stimulation baseline of sham and verum did not differ significantly [verum_pre vs. sham_pre: t = −0.152, p = .882 (paired t-test)].

There was no difference of the accuracy error after stimulation (all main factors and interactions n.s.).

3.2. Effects of tDCS on cortical activity and cortico-cortical coherence

In PD, the frequency domain spectrum (Fig. 3) over the sensorimotor area during motor task indicated activity modulation in a subrange of the high beta range from 22 to 27 Hz over the sensorimotor area that was considered for further analysis.

In PD, verum stimulation reduced activity (22-27 Hz) over the left sensorimotor area during the motor task (condition*group*session, F = 5.088, p = .015]. Since the power values did not show full normal distribution across all factors and domains, we recalculated the rmANOVA after log-transform of the power values (which resulted in normal distribution of the power data). This confirmed the significant interaction ('condition*group*session', F = 7.060, P = .006). In the post-hoc analysis we found that verum atDCS reduced activity from 22 to 27 Hz while it increased in sham (PD verum 'pre vs. post1': t = 2.652, p = .026 and PD sham 'pre vs. post2': t = −3.116, p = .012).

In PD, verum stimulation led to an additional right-hemispheric reduction of activity from 22 to 27 Hz during motor task (Fig. 4) (pre vs. post2, p = .0069) and this included the cluster of right centroparietal ('T4', 'T6', 'Cp6') and right frontotemporal areas ('F4', 'F8').

In contrast, PD patients showed an increase in beta activity after sham-stimulation [pre vs. post2, p = .0098] including the cluster of left sensorimotor and centroparietal areas ('T3', 'Cp5', 'Cp1', 'Cp2','Pz', 'P4') (Fig. 4).

In HC, there was no significant change in cortical activity after verum or sham stimulation [pre vs. post2, p = .07] (Fig. 5). For comparison, we found no significant modulation of beta activity ‚at rest'after either verum or sham stimulation, neither in PD nor in HC.

In terms of cortico-cortical coherence, we found in PD ‚motor task' an increase from 22-27Hz over the left sensorimotor area after verum-stimulation between ‚pre' and ‚post2' (cluster based permutation statistics 'pre vs. post2', p = .033 in Cp5, Cp1) (Fig. 6). This effect was not present in sham stimulation or in HC in neither verum nor sham. For comparison, we found no significant difference of cortico-cortical coherence ‚at rest'after verum stimulation, neither in PD nor in HC. In PD, we found a right-hemispheric increase of coherence after sham stimulation ‚at rest'(pre vs. post2, p = .029).

3.3. Disease-related characteristics of cortical activity and corticocortical coherence

To explore for disease-related characteristics in cortical activity and coherence, we compared the spectra between HC and PD in the 'pre' session. There was no difference of cortical activity between the groups before stimulation during motor task or 'at rest' from 22 to 27 Hz.

PD patients showed less cortico-cortical coherence between 'C3' and the central and right parieto-occipital areas ('Pz' 'P4' 'T6' 'O1') compared to HC during the motor task [cluster based permutation, independent samples t-test, p = .017] (Fig. 7). For comparison, no difference in cortico-cortical coherence was present 'at rest' between PD and HC.

4. Discussion

We characterized the effect of tDCS in Parkinson's disease on motor symptoms, fine motor performance, and cortical activity and synchronization measures. Verum atDCS modulated both cortical motor-network activity and synchronization from 22 to 27 Hz during a fine motor task. This was paralleled by clinical motor improvement. This finding was specific for the motor-task and carefully controlled against 'sham', 'rest' condition, and healthy matched controls. More specific, 'verum' atDCS decreased motor task specific activity from 22-27 Hz of the left sensorimotor and right frontal area. Furthermore, before stimulation PD patients presented with less cortico-cortical coherence over the left sensorimotor area during the motor task compared to HC. In terms of cortico-cortical synchronization, PD patients presented with decreased coherence of the left sensorimotor area when compared to HC before stimulation in the fine motor task. This was reversed by verum but not sham stimulation, i.e. synchronization of the PD sensorimotor area increased towards the level of HC. Together, our findings demonstrate that atDCS i) improves clinical motor outcome, and ii) specifically modulates the cortical motor network features depending on the combination of disease state and motor processing.

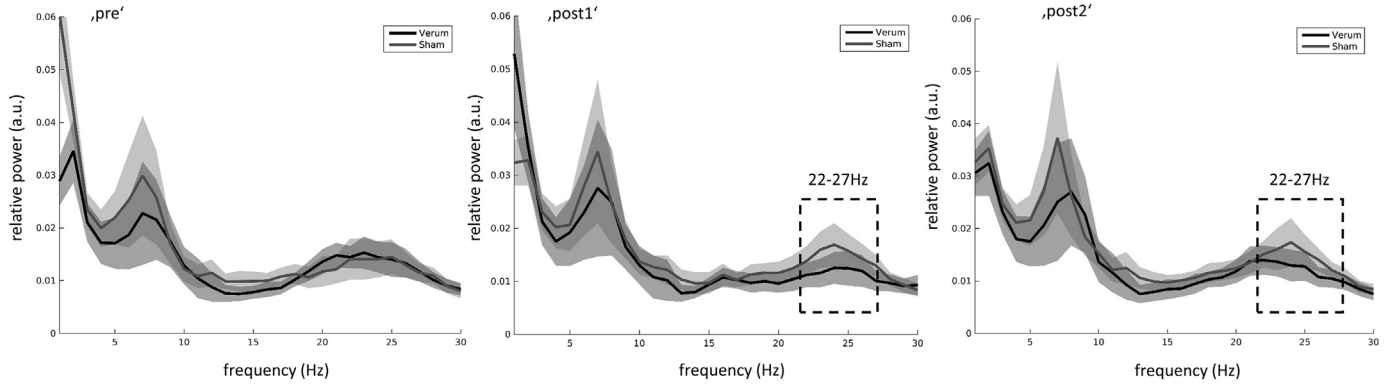

Fig. 3. Frequency domain activity over left sensorimotor area in PD.
Frequency domain activity over the left sensorimotor area ('C3') is given as grandaverage (error indicator given as standard error of the mean (shadow)) before ['pre'], directly after ['post1'] and 30 min after ['post2'] stimulation in either verum or sham condition. Verum condition (black line, standard error as dark grey shadow); sham condition (grey line, standard error as light grey shadow).

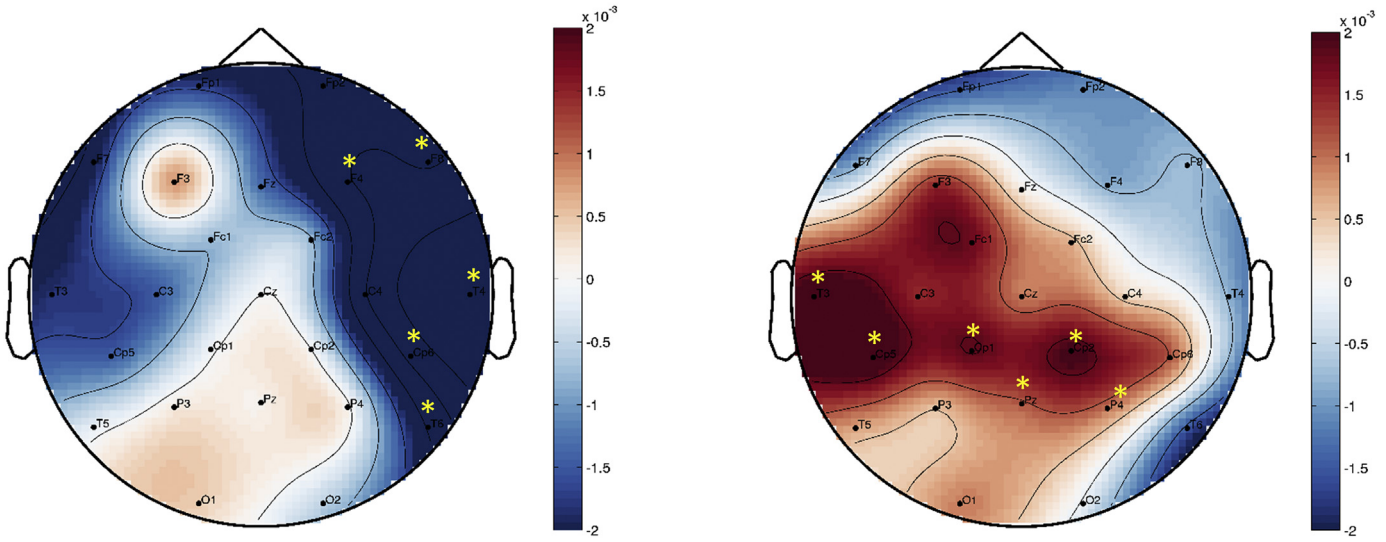

Fig. 4. Topographic distribution of frequency domain activity [22–27 Hz] in PD.
Difference plots (post2 - pre) of relative power with warm color indicating activity increase and cold color indicating activity reduction after stimulation. Asterisks indicate significant difference on cluster level. PD patients showed a significant decrease of activity after 'verum' stimulation [pre vs. post2, p = .0069] over the cluster of right centroparietal ['T4', 'T6', 'Cp6'] and right frontotemporal ['F4', 'F8'] areas, and a significant increase of activity after sham-stimulation [pre vs. post2, p = .0098] over the left sensorimotor and centroparietal areas ('T3', 'Cp5', 'Cp1', 'Cp2','Pz', 'P4').

4.1. Cortical network characteristics in PD and their modulation with effective atDCS

The topographic distribution of the widespread activity modulation from atDCS incorporated the left sensorimotor area and the right frontal area. Before stimulation, the left sensorimotor area showed similar activity from 22 to 27 Hz in both PD and HC both at rest and during motor task. Thus, the exaggerated oscillatory activity often observed on subthalamic level in the PD 'motor off' (Hammond et al., 2007) does not necessarily occur on cortical level. However, effective verum atDCS decreased cortical activity and, unlike sham, prevented a pathologic increase of activity. This activity modulation was confined to the motor task and absent at rest. Thus, the activity suppression from 22-27 Hz occurred in a rather specific situation of i) pathological PD motor OFF' i.e. after withdrawal of dopaminergic medication and ii) during 'fine motor integration'. Therefore, it did not reflect the PD motor 'OFF' and its modulation with effective neuromodulation in general but rather a movement-associated process comparable to beta activity decrease seen at onset and during phasic movement (Neuper et al., 2006). The combination of motor and rest conditions and a control group in this study helps to gain further insight into cortical beta characteristics and may extend the findings from subthalamic LFP research, in which HCs are not available. It adds to the previous perspective that therapeutic beta amplitude modulation not only associates to a certain disease state

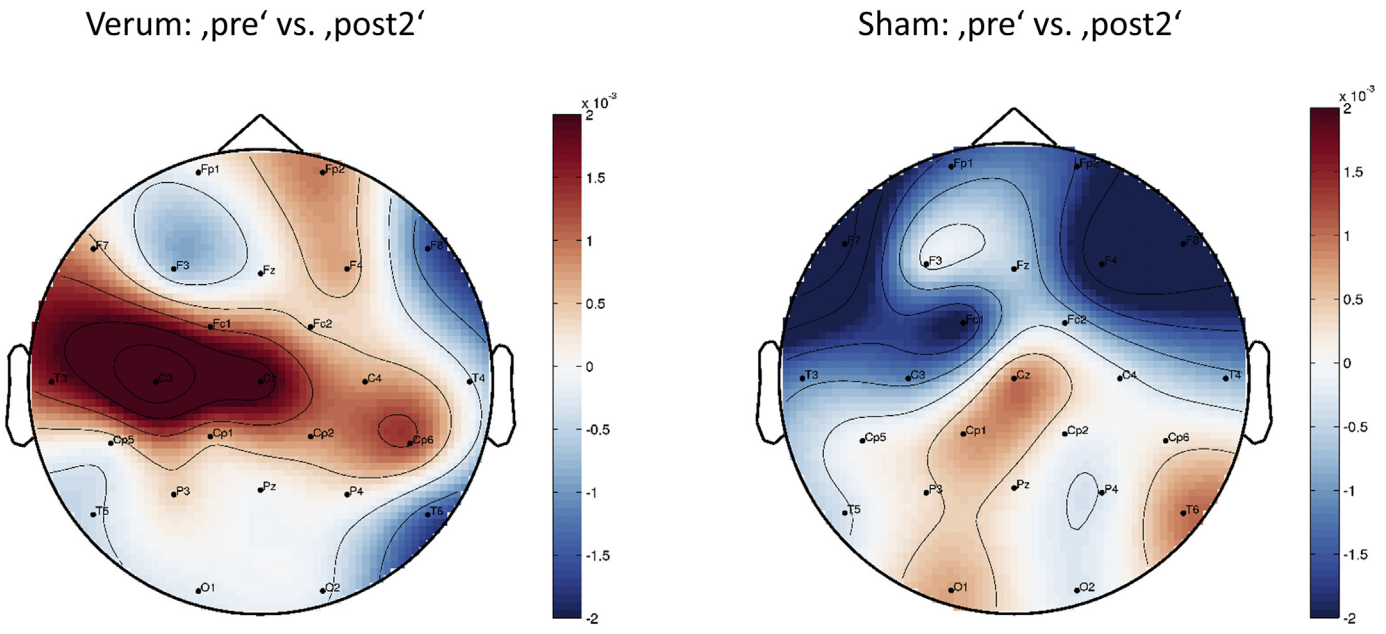

Fig. 5. Topographic distribution of frequency domain activity [22-27 Hz] in HC.

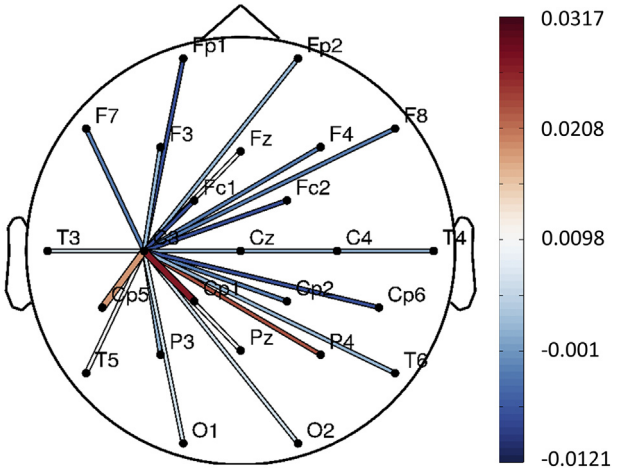

Fig. 6. Corticocortical coherence.
Imaginary corticocortical coherence [22–27 Hz] of left sensorimotor area (C3) to all other electrodes in PD. PD patients showed a significant increase of coherence from C3 to Cp5 and Cp1 (represented by thick lines) over the left primary motor area 30 min after 'verum' stimulation ('post2') compared to before stimulation ('pre'). No other connectivity reached significance. This connected topoplot shows the difference of coherence between ‚post2' and ‚pre' [post2-pre] (color-coded) with results from cluster-based permutations statistic [pre vs. post2, p = 0.033]. These effects were specific for the PD 'verum' condition and absent in both PD 'sham' and in healthy controls 'verum' and 'sham' conditions.

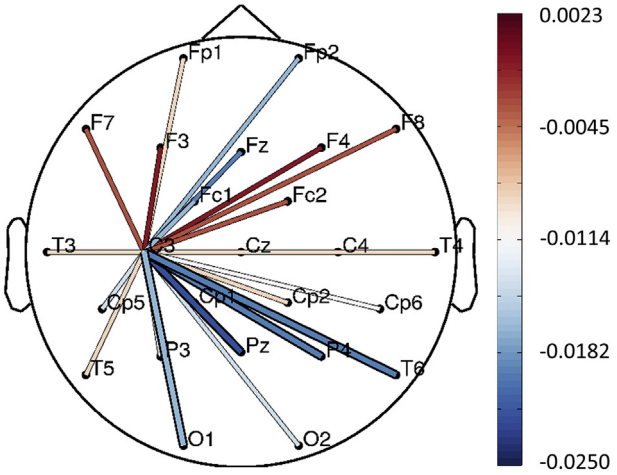

Fig. 7. Disease related differences in corticocortical coherence.
Imaginary corticocortical coherence [22–27 Hz] of left motor area (C3) to all other electrodes comparing PD patients with HC before stimulation. The figure shows a connected topoplot of the difference between PD and HC in the 'pre' session (after averaging 'pre' verum and 'pre' sham for both groups). PD patients show significantly less cortico-cortical coherence between 'C3' and the central and right parieto-occipital areas ('P4','Pz','T6','O1'). No other connectivity reached significance. Thick lines represent these significant channels on cluster level.

(Tinkhauser et al., 2017a; Pogosyan et al., 2009; Brittain and Brown, 2014) – but may in addition depend on cognitive network functions - here fine motor integration. This interpretation is plausible, given that manifold cortical and subcortical processes modulate the sensorimotor area (SM1), e.g. in terms of movement planning and preparation upon frontal executive functioning (Weiss et al., 2015; Pfurtscheller, 2000; George et al., 2013).

With respect to the SM1, our observation of beta amplitude suppression with verum atDCS is in line with previous work using different brain stimulation methods. To our knowledge, there is no previous data of beta activity modulation with atDCS in PD and HC. However, clinically effective subthalamic stimulation reduced movement-related beta oscillations in PD over the bilateral SM1 areas and further included the right frontal area (Weiss et al., 2015; Whitmer et al., 2012). In addition, cortical M1 TMS reversely modulated subthalamic beta band oscillations (Gaynor et al., 2008). These studies provide evidence of direct cortical coupling and reciprocal access to the pathological subcortico-cortical beta-related motor network.

Furthermore, a study using transcranial alternating current stimulation (tACS) showed an opposed clinical effect with slowing of movement when beta oscillations were entrained with 20 Hz tACS stimulation. Together, this underlines the relevance of cortical beta activity modulation for PD motor performance (Pogosyan et al., 2009).

Apart from activity modulation over the SM1, we found activity reduction over the right frontal area from 22 to 27 Hz. The prefrontal cortex is involved in executive motor function and seems to process motor inhibition like the suppression of motor tasks (Brittain et al., 2012; Aron and Poldrack, 2006; Aron et al., 2004; Aron et al., 2014), as well as response selection in attention-demanding motor skills (Jahanshahi, 2013). More specific to PD, increased beta activity over the right frontal cortex occurs in successful 'stopping' and supports inhibitory motor control (George et al., 2013). As endogenous inhibitory motor signals may be transmitted in beta bursts in cortical networks (Picazio et al., 2014), a reduction of beta activity in this area may facilitate movement through disinhibition of executive motor preparation. Here, the ipsi- and contralateral activity changes might indicate modulation of interconnected areas. The remarkable topographic similarity of motor network modulation compared to our DBS work (Weiss et al., 2015) may suggest shared network nodes linking the left SM1 as well as the right frontal area. This might compare to the hyperdirect pathway, which links the STN to the pre-supplementary motor area and the right inferior frontal area (Aron et al., 2014).

With respect to cortico-cortical synchronization, we found that cortico-cortical coherence was reduced over the left SM1 area in PD before stimulation when compared to HC. The fact, that 'verum atDCS' enhanced local cortico-cortical synchronization, seems – at first glance – to be at odds with existing findings from subthalamic synchronization. On subthalamic level, the enhanced local synchronization generally mirrored the pathological disease state. Whether this also applies to subthalamo – M1 or cortico-cortical synchronization remains controversial.

In this framework, our findings give a closer characterization of cortico-cortical synchronization from 22 to 27 Hz in PD. From our findings, it is unlikely that cortico-cortical synchronization purely reflects disease-related motor network states and that atDCS exclusively interferes with this. Rather, we suggest a motor-task specific dysregulation of the PD motor network. Notably, when comparing this finding to the literature on PD patients with subthalamic recordings, it has to be kept in mind that our cohort was less advanced in disease. Therefore, we cannot exclude that our patients would still have greater compensatory reserve to hinder cortical upregulation of beta activity in general.

Furthermore, the increase of cortico-cortical coherence occurred under fine motor performance. In context with existing work on fine motor integration, higher coherence in the SM1 area seems useful to stabilize neuronal integration of isometric fine motor performance (Kristeva et al., 2007). As such, isometric contraction relates to higher cortico-spinal coherence and associates with stable motor output and higher precision in previous work (Kristeva et al., 2007). Coupling between the primary motor cortex and the spinal motor neurons occurred at 20 Hz and may represent the central drive from motor cortex to the motor neuron firing (Gross et al., 2000; Salenius et al., 1997).

In addition, the effect of atDCS in our work may underpin, that the Parkinsonian cortex is susceptible to excitability modulation with atDCS under motor conditions. More speculative and hypothesis-generating for future work, this might reflect the cortical potential to compensate for subcortical processing failure (by altering cortical

synaptic transmission) along emerging, progressive neurodegeneration.

4.2. Methodological considerations

The findings in this study were carefully controlled, and the study protocol had high clinical standards in choosing a randomized and double-blind stimulation protocol. However, this is not to withstand, that limitations exist in this study. In general, we would have preferred a larger set of cortical electrodes in order to enable cortical source reconstructions. However, this was not possible with this combined tDCS-EEG montage that yielded the possibility to place the C3 electrode within the cortical anodal ring electrode. This also had advantages, i.e. to leave the recording and stimulation electrode setting constant in place over the whole experimental session. Inherently, atDCS may lead to widespread modulation of neural activity (Polania et al., 2011) depending on several factors such as the activity of the underlying tissue or axonal spatial orientation (Manola et al., 2005; Kabakov et al., 2012). Thus, the constant electrode arrangement over the whole session will be advantageous to minimize the influence of such confounders. In addition, it provided the possibility for simultaneous EEG recording during the active stimulation session, which we plan to report as separate work.

4.3. Conclusion

This study sheds light on cortical oscillatory features of PD fine motor integration and functional mechanisms of tDCS. We found that the PD motor network was susceptible to atDCS during fine motor performance in attenuating cortical oscillatory activity and fostering cortico-cortical synchronization. It delineated that cortical oscillatory features are not in general and 'per se' altered in pathological disease conditions like PD, but may strongly depend on a combination of disease state and context, e.g. integration of motor processing.

Declarations of interest

None.

Anna Schoellmann, Marlieke Scholten, Barbara Wasserka, Rathinaswamy B Govindan, Rejko Krüger, Alireza Gharabaghi, Christian Plewnia and Daniel Weiss declare no competing financial interests. This research did not receive any specific grant from funding agencies in the public, commercial, or not-for-profit sectors.

D. Weiss is supported by the German Research Council (WE5375/1-1) and the Michael J Fox Foundation; received speakers' honoraria and travel grants from Medtronic, Abbott/St Jude, Boston Scientific; consultant for STADA pharma. C. Plewnia receives funding by the German Federal Ministry of Education and Research (research consortia ESPRIT / FKZ 01EE1407H and GCBS / FKZ 01EE1403D) and the German Research Council (DFG: PL 525/4-1; PL 525/6-1; PL 525/7-1).

Acknowledgements

None.

Difference plots (post2 - pre) of relative power with warm color indicating activity increase and cold color indicating activity reduction after stimulation. We found no significant change in cortical beta activity after verum- or sham-stimulation (verum pre vs. post2, p = .07, sham pre vs. post 2, p = 1) in healthy controls on cluster level.

References

Ambrus, G.G., et al., 2012. The fade-in–short stimulation–fade out approach to sham tDCS–reliable at 1 mA for naive and experienced subjects, but not investigators. Brain Stimul. 5 (4), 499–504.
Aron, A.R., Poldrack, R.A., 2006. Cortical and subcortical contributions to stop signal response inhibition: role of the subthalamic nucleus. J. Neurosci. 26 (9), 2424–2433.
Aron, A.R., Robbins, T.W., Poldrack, R.A., 2004. Inhibition and the right inferior frontal cortex. Trends Cogn. Sci. 8 (4), 170–177.
Aron, A.R., Robbins, T.W., Poldrack, R.A., 2014. Inhibition and the right inferior frontal cortex: one decade on. Trends Cogn. Sci. 18 (4), 177–185.
Baudewig, J., et al., 2001. Regional modulation of BOLD MRI responses to human sensorimotor activation by transcranial direct current stimulation. Magn. Reson. Med. 45 (2), 196–201.
Beck, A.T., et al., 1996. Comparison of beck depression inventories -IA and -II in psychiatric outpatients. J. Pers. Assess. 67 (3), 588–597.
Benninger, D.H., Hallett, M., 2015. Non-invasive brain stimulation for Parkinson's disease: current concepts and outlook 2015. NeuroRehabilitation 37 (1), 11–24.
Benninger, D.H., et al., 2010. Transcranial direct current stimulation for the treatment of Parkinson's disease. J. Neurol. Neurosurg. Psychiatry 81 (10), 1105–1111.
Brittain, J.S., Brown, P., 2014. Oscillations and the basal ganglia: motor control and beyond. NeuroImage 85 (Pt 2), 637–647.
Brittain, J.S., et al., 2012. A role for the subthalamic nucleus in response inhibition during conflict. J. Neurosci. 32 (39), 13396–13401.
Brown, P., 2007. Abnormal oscillatory synchronisation in the motor system leads to impaired movement. Curr. Opin. Neurobiol. 17 (6), 656–664.
Costa-Ribeiro, A., et al., 2016. Dopamine-independent effects of combining transcranial direct current stimulation with cued gait training on cortical excitability and functional mobility in Parkinson's disease. J. Rehabil. Med. 48 (9), 819–823.
Costa-Ribeiro, A., et al., 2017. Transcranial direct current stimulation associated with gait training in Parkinson's disease: a pilot randomized clinical trial. Dev. Neurorehabil. 20 (3), 121–128.
Dagan, M., et al., 2018. Multitarget transcranial direct current stimulation for freezing of gait in Parkinson's disease. Mov. Disord. 33 (4), 642–646.
Delorme, A., Makeig, S., 2004. EEGLAB: an open source toolbox for analysis of single-trial EEG dynamics including independent component analysis. J. Neurosci. Methods 134 (1), 9–21.
Eusebio, A., et al., 2011. Deep brain stimulation can suppress pathological synchronisation in parkinsonian patients. J. Neurol. Neurosurg. Psychiatry 82 (5), 569–573.
Ferrucci, R., et al., 2016. Cerebellar and motor cortical transcranial stimulation decrease levodopa-induced dyskinesias in Parkinson's disease. Cerebellum 15 (1), 43–47.
Floel, A., 2014. tDCS-enhanced motor and cognitive function in neurological diseases. NeuroImage 85 (Pt 3), 934–947.
Folstein, M.F., Folstein, S.E., McHugh, P.R., 1975. "Mini-mental state". A practical method for grading the cognitive state of patients for the clinician. J. Psychiatr. Res. 12 (3), 189–198.
Francis, J.T., Gluckman, B.J., Schiff, S.J., 2003. Sensitivity of neurons to weak electric fields. J. Neurosci. 23 (19), 7255–7261.
Fregni, F., et al., 2006. Transient tinnitus suppression induced by repetitive transcranial magnetic stimulation and transcranial direct current stimulation. Eur. J. Neurol. 13 (9), 996–1001.
Gaynor, L.M., et al., 2008. Suppression of beta oscillations in the subthalamic nucleus following cortical stimulation in humans. Eur. J. Neurosci. 28 (8), 1686–1695.
George, J.S., et al., 2013. Dopaminergic therapy in Parkinson's disease decreases cortical beta band coherence in the resting state and increases cortical beta band power during executive control. Neuroimage Clin. 3, 261–270.
Gross, J., et al., 2000. Cortico-muscular synchronization during isometric muscle contraction in humans as revealed by magnetoencephalography. J. Physiol. 527 (Pt 3), 623–631.
Hammond, C., Bergman, H., Brown, P., 2007. Pathological synchronization in Parkinson's disease: networks, models and treatments. Trends Neurosci. 30 (7), 357–364.
Hjorth, B., 1991. Principles for transformation of scalp EEG from potential field into source distribution. J. Clin. Neurophysiol. 8 (4), 391–396.
Jahanshahi, M., 2013. Effects of deep brain stimulation of the subthalamic nucleus on inhibitory and executive control over prepotent responses in Parkinson's disease. Front. Syst. Neurosci. 7, 118.
Kabakov, A.Y., et al., 2012. Contribution of axonal orientation to pathway-dependent modulation of excitatory transmission by direct current stimulation in isolated rat hippocampus. J. Neurophysiol. 107 (7), 1881–1889.
Kayser, J., Tenke, C.E., 2015. Issues and considerations for using the scalp surface Laplacian in EEG/ERP research: a tutorial review. Int. J. Psychophysiol. 97 (3), 189–209.
Keeser, D., et al., 2011a. Prefrontal transcranial direct current stimulation changes connectivity of resting-state networks during fMRI. J. Neurosci. 31 (43), 15284–15293.
Keeser, D., et al., 2011b. Prefrontal direct current stimulation modulates resting EEG and event-related potentials in healthy subjects: a standardized low resolution tomography (sLORETA) study. NeuroImage 55 (2), 644–657.
Klem, G.H., et al., 1999. The ten-twenty electrode system of the international federation. The international federation of clinical neurophysiology. Electroencephalogr. Clin. Neurophysiol. Suppl. 52, 3–6.
Kristeva, R., Patino, L., Omlor, W., 2007. Beta-range cortical motor spectral power and corticomuscular coherence as a mechanism for effective corticospinal interaction during steady-state motor output. NeuroImage 36 (3), 785–792.
Kuhn, A.A., et al., 2006. Reduction in subthalamic 8-35 Hz oscillatory activity correlates with clinical improvement in Parkinson's disease. Eur. J. Neurosci. 23 (7), 1956–1960.
Kuhn, A.A., et al., 2008. High-frequency stimulation of the subthalamic nucleus suppresses oscillatory beta activity in patients with Parkinson's disease in parallel with improvement in motor performance. J. Neurosci. 28 (24), 6165–6173.
Lalo, E., et al., 2008. Patterns of bidirectional communication between cortex and basal ganglia during movement in patients with Parkinson disease. J. Neurosci. 28 (12), 3008–3016.
Lang, N., et al., 2005. How does transcranial DC stimulation of the primary motor cortex alter regional neuronal activity in the human brain? Eur. J. Neurosci. 22 (2),

495–504.
Lefaucheur, J.P., et al., 2004. Improvement of motor performance and modulation of cortical excitability by repetitive transcranial magnetic stimulation of the motor cortex in Parkinson's disease. Clin. Neurophysiol. 115 (11), 2530–2541.
Lefaucheur, J.P., et al., 2017. Evidence-based guidelines on the therapeutic use of transcranial direct current stimulation (tDCS). Clin. Neurophysiol. 128 (1), 56–92.
Litvak, V., et al., 2011. Resting oscillatory cortico-subthalamic connectivity in patients with Parkinson's disease. Brain 134 (Pt 2), 359–374.
Manola, L., et al., 2005. Modelling motor cortex stimulation for chronic pain control: electrical potential field, activating functions and responses of simple nerve fibre models. Med. Biol. Eng. Comput. 43 (3), 335–343.
Maris, E., 2012. Statistical testing in electrophysiological studies. Psychophysiology 49 (4), 549–565.
Maris, E., Oostenveld, R., 2007. Nonparametric statistical testing of EEG- and MEG-data. J. Neurosci. Methods 164 (1), 177–190.
McAuley, J.H., Rothwell, J.C., Marsden, C.D., 1997. Frequency peaks of tremor, muscle vibration and electromyographic activity at 10 Hz, 20 Hz and 40 Hz during human finger muscle contraction may reflect rhythmicities of central neural firing. Exp. Brain Res. 114 (3), 525–541.
Neuper, C., Wortz, M., Pfurtscheller, G., 2006. ERD/ERS patterns reflecting sensorimotor activation and deactivation. Prog. Brain Res. 159, 211–222.
Nitsche, M.A., Paulus, W., 2000. Excitability changes induced in the human motor cortex by weak transcranial direct current stimulation. J. Physiol. 527 (Pt 3), 633–639.
Nitsche, M.A., Paulus, W., 2001. Sustained excitability elevations induced by transcranial DC motor cortex stimulation in humans. Neurology 57 (10), 1899–1901.
Nitsche, M.A., et al., 2003. Safety criteria for transcranial direct current stimulation (tDCS) in humans. Clin. Neurophysiol. 114 (11), 2220–2222 (author reply 2222-3).
Nolte, G., et al., 2004. Identifying true brain interaction from EEG data using the imaginary part of coherency. Clin. Neurophysiol. 115 (10), 2292–2307.
Oldfield, R.C., 1971. The assessment and analysis of handedness: the Edinburgh inventory. Neuropsychol. 9 (1), 97–113.
Oostenveld, R., et al., 2011. FieldTrip: open source software for advanced analysis of MEG, EEG, and invasive electrophysiological data. Comput. Intell. Neurosci. 2011, 156869.
Oswal, A., et al., 2016. Deep brain stimulation modulates synchrony within spatially and spectrally distinct resting state networks in Parkinson's disease. Brain 139 (Pt 5), 1482–1496.
Palm, U., et al., 2013. Evaluation of sham transcranial direct current stimulation for randomized, placebo-controlled clinical trials. Brain Stimul. 6 (4), 690–695.
Pascual-Leone, A., et al., 1994. Akinesia in Parkinson's disease. II. Effects of subthreshold repetitive transcranial motor cortex stimulation. Neurology 44 (5), 892–898.
Pfurtscheller, G., 2000. Spatiotemporal ERD/ERS patterns during voluntary movement and motor imagery. Suppl. Clin. Neurophysiol. 53, 196–198.
Pfurtscheller, G., Lopes, F.H., 1999. da Silva, Event-related EEG/MEG synchronization and desynchronization: basic principles. Clin. Neurophysiol. 110 (11), 1842–1857.
Picazio, S., et al., 2014. Prefrontal control over motor cortex cycles at beta frequency during movement inhibition. Curr. Biol. 24 (24), 2940–2945.
Pogosyan, A., et al., 2009. Boosting cortical activity at Beta-band frequencies slows movement in humans. Curr. Biol. 19 (19), 1637–1641.
Polania, R., Nitsche, M.A., Paulus, W., 2011. Modulating functional connectivity patterns and topological functional organization of the human brain with transcranial direct current stimulation. Hum. Brain Mapp. 32 (8), 1236–1249.
Polania, R., Paulus, W., Nitsche, M.A., 2012. Modulating cortico-striatal and thalamo-cortical functional connectivity with transcranial direct current stimulation. Hum. Brain Mapp. 33 (10), 2499–2508.
Potter-Nerger, M., et al., 2008. Subthalamic nucleus stimulation restores corticospinal facilitation in Parkinson's disease. Mov. Disord. 23 (15), 2210–2215.
Priori, A., et al., 1998. Polarization of the human motor cortex through the scalp. Neuroreport 9 (10), 2257–2260.
Roy, A., Baxter, B., He, B., 2014. High-definition transcranial direct current stimulation induces both acute and persistent changes in broadband cortical synchronization: a simultaneous tDCS-EEG study. IEEE Trans. Biomed. Eng. 61 (7), 1967–1978.
Salenius, S., et al., 1997. Cortical control of human motoneuron firing during isometric contraction. J. Neurophysiol. 77 (6), 3401–3405.
Santarnecchi, E., et al., 2014. Time course of corticospinal excitability and autonomic function interplay during and following monopolar tDCS. Front Psychiatry 5, 86.
Silberstein, P., et al., 2005. Cortico-cortical coupling in Parkinson's disease and its modulation by therapy. Brain 128 (Pt 6), 1277–1291.
Tinkhauser, G., et al., 2017a. The modulatory effect of adaptive deep brain stimulation on beta bursts in Parkinson's disease. Brain 140 (4), 1053–1067.
Tinkhauser, G., et al., 2017b. Beta burst dynamics in Parkinson's disease OFF and ON dopaminergic medication. Brain 140 (11), 2968–2981.
Tinkhauser, G., et al., 2018. Beta burst coupling across the motor circuit in Parkinson's disease. Neurobiol. Dis. 117, 217–225.
Trenado, C., et al., 2014. Enhanced corticomuscular coherence by external stochastic noise. Front. Hum. Neurosci. 8, 325.
Uhlhaas, P.J., Singer, W., 2006. Neural synchrony in brain disorders: relevance for cognitive dysfunctions and pathophysiology. Neuron 52 (1), 155–168.
Valentino, F., et al., 2014. Transcranial direct current stimulation for treatment of freezing of gait: a cross-over study. Mov. Disord. 29 (8), 1064–1069.
van Wijk, B.C., et al., 2016. Subthalamic nucleus phase-amplitude coupling correlates with motor impairment in Parkinson's disease. Clin. Neurophysiol. 127 (4), 2010–2019.
Verheyden, G., et al., 2013. Immediate effect of transcranial direct current stimulation on postural stability and functional mobility in Parkinson's disease. Mov. Disord. 28 (14), 2040–2041.
Weiss, D., et al., 2012. Subthalamic nucleus stimulation restores the efferent cortical drive to muscle in parallel to functional motor improvement. Eur. J. Neurosci. 35 (6), 896–908.
Weiss, D., et al., 2015. Subthalamic stimulation modulates cortical motor network activity and synchronization in Parkinson's disease. Brain 138 (Pt 3), 679–693.
Whitmer, D., et al., 2012. High frequency deep brain stimulation attenuates subthalamic and cortical rhythms in Parkinson's disease. Front. Hum. Neurosci. 6, 155.
Wichmann, T., et al., 2011. Milestones in research on the pathophysiology of Parkinson's disease. Mov. Disord. 26 (6), 1032–1041.